NCNE-2020 Special Issue

J. Indian Chem. Soc.,
Vol. 97, July 2020, pp. 1119-1123

Optimizing hydrodynamic forces for gypsum scale removal and analysis through modelling using COMSOL

Shahid Z. Ansari[a], Anjali A. Ingle[b], Diwakar Z. Shende[b] and Aniruddha B. Pandit*[a]

[a]Department of Chemical Engineering, Institute of Chemical Technology, Mumbai-40019, India

[b]ASAL, Department of Chemical Engineering, Vidyasagar National Institute of Technology, Nagpur-440 010, Maharashtra, India

E-mail: ab.pandit@ictmumbai.edu.in

Manuscript received online 07 April 2020, accepted 12 June 2020

Metal salts deposition on the surfaces of heat transfer equipment is one of the critical problems faced in chemical industries. A slight change in operating parameters of the process fluid after coming in contact with a foreign surface or particle often results in equilibrium shift of the dissolved metal ions leading to scale deposition. This causes reduced thermal efficiency, high maintenance cost and increased pressure drop in the unit has been observed followed by plant shut down for maintenance.

The present work involves a systematic simulation and modelling of a Stirred Tank Reactor (STR) with different orientations of the impeller. The effect of the fluid flow and hydrodynamic condition on surface of the impellers was studied and compared with experimental values from literature to confirm its significance on gypsum scale deposition or removal from the metal surface. The system was modelled using multiphysics software COMSOL version 5 for understanding of the process. It was observed that on increasing Reynolds number (*Re*), linear tip velocity (*V*) and shear rate (s^{-1}) of the fluid, the rate of scale deposition increased up to Re of 21,000, V of 3.5–4 m/s and s of 25–33 1/s respectively. However, beyond these values the rate of scale formation and deposition started reducing and further increase in these parameters leads to physical attrition of the metal surface.

Keywords: Gypsum scale, inhibition, COMSOL, erosion, Reynolds number.

Introduction

Scale deposition is one of the major problem in industries where heat transfer equipments or water are used for heat transfer from hot to cold fluid or vice versa. Conventionally, there are different methods to counter attack the phenomenon of scale deposition. The process of scale deposition can be significantly reduced by adding additives like sodium hexametaphosphate, polyacrylic acid, polymalic acid, polyepoxysuccinic acid, polyaspsartic acid etc. to the fluid[1–3]. Magnetic treatment of the dissolved metals ions present in the fluid or by changing the properties of the fluid etc.[4,5]. However, these techniques are ineffective and relatively costly. Addition of sulphur, phosphorous and nitrogen rich additives in the water bodies leads to eutrophication of water bodies and disturbs the ecosystem[3,6–8].

The phenomenon of scale deposition is largely observed in the pipelines of the process water in industries. The process of scale deposition is due to presence of adhesive force of attraction between the metal surface and the crystal particles. If in some or the other way, this adhesive force is overcome by applying external shear force on the deposited particles, the crystals can be effectively removed from the metal surface and the process of scale deposition can be reduced or avoided significantly[2,9,10]. This shear force on the settled crystals can be applied by the fluid inside the pipe itself, hence by optimizing this shear force of the fluid on the crystals, the process of scaling can be effectively controlled and inhibited. Studying the process of scale deposition in pipes on lab scale is a lot cumbersome. However, the fluid conditions in a pipe can be mimicked or imitated using a Stirred Tank Reactor[11]. Limited experimental work has been done in literature to establish the relation between the Reynolds number and the rate of scale deposition on cylindrical and rectangular metal coupons[12–15]. However, predicting the rate of scale deposition alone on the basis of Reynolds number is insufficient and cannot be accounted for. Hence, there is a greater need to study the effect of different parameter i.e. shear rate, energy dissipation etc. on the process of scale deposition[11,16].

The present study focusses on modelling and simulating a Stirred Tank Reactor (STR) with different orientation of the impeller to observe the effect of Reynolds number, linear tip velocity, turbulence, shear rate and eddies on the process of salt deposition on the surface of the impeller. By doing so, the effect of various hydrodynamic parameter on scale deposition and inhibition can be predicted easily without much dependence on the experimental data backups. Same impellers with different orientations (i.e. Disc and Paddle) as shown in Fig. 1 was used.

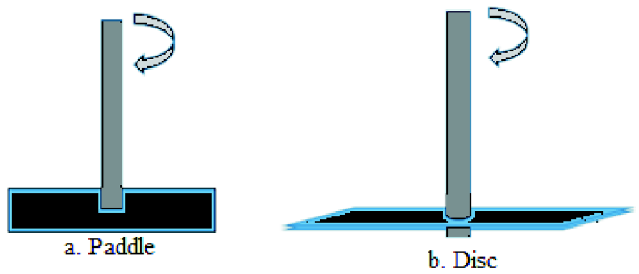

Fig. 1. Orientation of the impellers.

The outcomes achieved through this study was compared with the experimental values from the literature[11].

Mathematical modelling:

The desired stirred tank system for the study was modelled and simulated in multiphysics software COMSOL version 5, to observe the results of operating parameters on the surface. Similar study of the hydrodynamic parameters on the surface of the impeller of a stirred tank vessel is studied in various works[16–20].

The different operating parameters i.e. Reynolds number, linear tip velocity, shear rate can be estimated from the following relations.

Paddle and disc type impeller:

Reynolds number of the fluid in a STR is a function of the diameter of the impeller, rpm, density and viscosity of the fluid. So changing the impeller orientation, Reynolds number remains the same, however degree of turbulence in the two cases varies significantly. Using the impeller as paddle higher proportion of energy is dissipated in the form of turbulent kinetic energy and remaining smaller part is dispersed for creating linear velocity in the fluid bulk and vice versa when the impeller is used as disc.

Reynolds number is given by the relation[11,21,22],

$$Re = \frac{ND^2\varrho}{\mu} \tag{1}$$

where,

$$N\,(\text{rps}) = \frac{\nu}{2\times\pi\times r} \tag{2}$$

ν = linear tip velocity (m/s), D = diameter of impeller (m), μ = viscosity (kg/m.s) and ϱ = density of the solution (kg/m^3).

The power required is calculated using the following relation,

$$P = NpN^3D^5\varrho \tag{3}$$

where $$Np = \frac{A}{Re} + B\frac{(10^3 + 0.6fRe^a)^p}{(10^3 + 1.6fRe^a)^p}$$

is the power number (Np) and p, A and B is governed by the impeller geometry[21,22].

Shear rate:

The shear rate can be estimated by the following correlation from the above equations[11,16],

$$\gamma = \sqrt{\frac{1P}{\mu V}} \tag{4}$$

Eq. (9) is applicable to all types of flow, further, power number is related to Reynolds number as,

$$Np = \frac{C}{Re} \tag{5}$$

Analysis of dynamics of the STR by finite element method:

The assumptions made while modelling the systems were that the fluid in incompressible and conditions were steady state.

The dynamics of the system was defined by the following governing equations,

$$\rho(u\cdot\nabla)u = \nabla\cdot[-\rho I + K] + F] \quad (6)$$

$$\rho\nabla\cdot(u) = 0 \quad (7)$$

$$K = [(\mu + \mu_T)(\nabla u + (\nabla u)^T)] \quad (8)$$

$$Re_w = \frac{\rho u l_w}{\mu} \quad (9)$$

$$\nabla G\cdot\nabla G + \sigma_w G(\nabla\cdot\nabla G) = (1 + 2\sigma_w)G^4 \quad (10)$$

$$l_w = \frac{1}{G} - \frac{l_{ref}}{2} \quad (11)$$

$$\mu_T = \mu\left(\left(\frac{df}{dl_w^+}\right)^{-1}\right) - 1 \quad (12)$$

Boundary conditions:

The boundary conditions given to different domains of the modelled system were as follows:

Boundary conditions for the tank wall was given by eq. (13) and rotating wall by eqs. (14) and (15),

$$u = 0 \quad (13)$$

$$u = v_{wall} \quad (14)$$

$$\left(\frac{\partial_w}{\partial_t}\right)_x = v_{wall} \quad (15)$$

Boundary condition for Rotating domain i.e. for the impeller is given by eq. (16).

$$dx = dx\,(r_{bp}, \omega, r) \quad (16)$$

Geometry and mesh:

The tetrahedron mesh system for the geometry was build using finite element method as can be seen in Fig. 2. Fine meshing was done as mesh number and mesh type play a vital role in calculation of efficiency and accuracy. In 88% of the overall STR volume of STR tetrahedron mess is used. The MEQ (Minimum Element Quality) was 0.01007 and AEQ (Average Element Quality) was 0.6803.

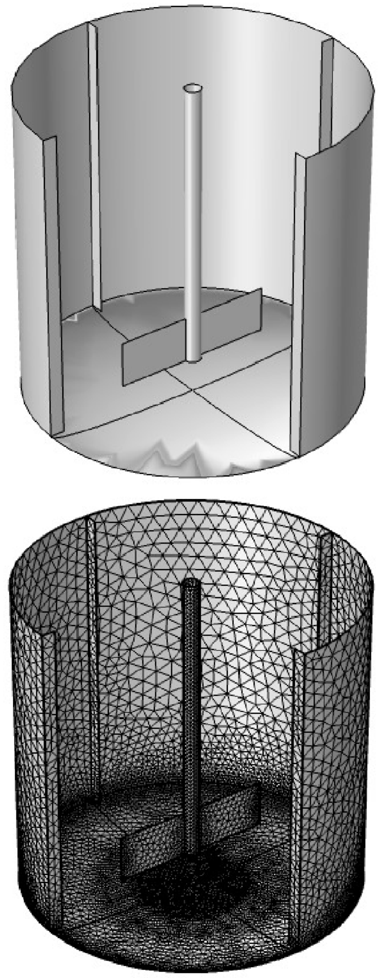

Fig. 2. Geometry and mesh of the system in COMSOL.

Results and discussion

Experimental studies confirmed that increasing the linear tip velocity of different type of impellers, the rate of scale deposition was found to be growing up to certain value and beyond this limit it started declining. This optimum value of linear tip velocity for disc type impeller was estimated to be 1 m/s and for paddle type impeller this value was around 0.5–0.7 m/s. Complete scale inhibition on the surface of the metal coupons was observed to be around 3.8-4 m/s and 1 m/s for Disc and Paddle type impellers respectively. At this point, calculated Reynolds number for the respective impellers at which the rate of scale deposition was completely avoided was found to be above 80,000 and 21,000 respectively[11].

Analyzing the simulation outcomes shown that increase in the Reynolds number triggered an increase in the shear rate by the fluid on the metal surface. The shear rate was observed to be maximum at the surface of the impeller and it went on reducing radially towards the vessel wall as seen in Fig. 3. The amount of shear rate on the metal surface of the impeller was significantly higher in Paddle type as compared to Disc impeller. At similar Reynolds number the degree of

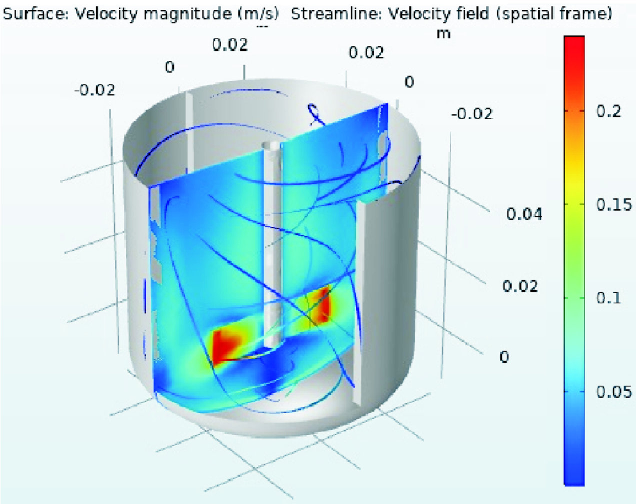

Fig. 3a. Radial velocity distribution profile at 120 rpm.

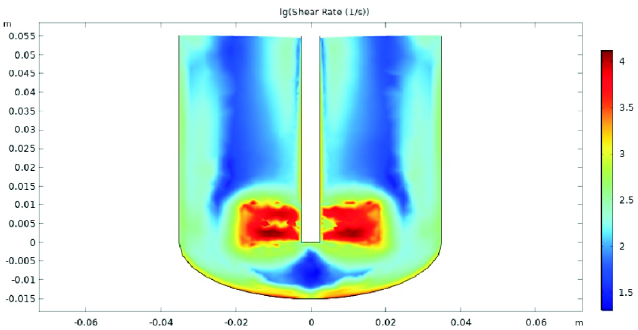

Fig. 3b. Radial shear rate distribution at 120 rpm.

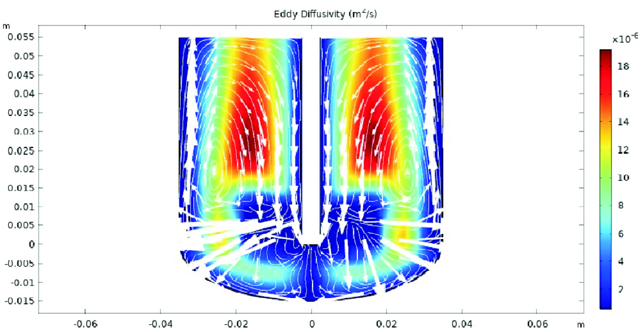

Fig. 3c. Radial eddy diffusivities in the liquid bulk at 120 rpm.

turbulence in Paddle type impeller was observed to be higher as compared to Disc type impeller. In other words, higher proportion of the overall dissipated energy was released to generate turbulence in the vessel where impeller is used as paddle and lower amount of energy is released to create linear velocity of the bulk fluid. Similarly, when the disc type impeller was used it was observed that substantial amount of energy is dispersed to create linear velocity in the fluid bulk and lesser proportion of energy is dispersed to create turbulence. At Reynolds number of 21,000 or tip velocity of 1 m/s the maximum shear rate at the metal surface was about 24–35 s^{-1} for Paddle and Disc type impellers. Hence, it was observed that maintaining the shear rate in the range of 24–35 s^{-1}, the process of scale deposition can be minimized or inhibited completely. However, further increase in the shear rate beyond this range enhances the process of metal erosion by the shear rate due to fluid flow.

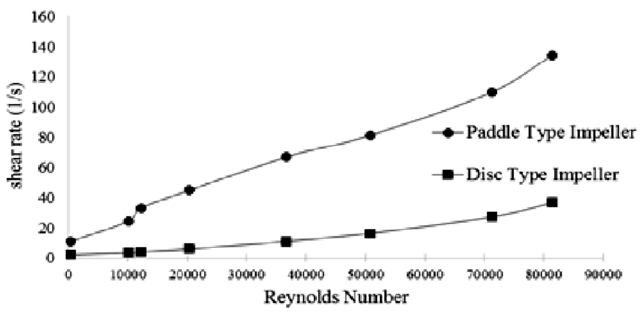

Fig. 4. Shear rate at different linear tip velocity for Paddle and Disc type impeller.

Conclusion

The study revealed that turbulence boosts the process of scale deposition up to certain limit and beyond this limit it circumvents the scale deposition and further increase in the turbulence or shear rate leads to metal erosion. The optimized operating conditions for scale inhibition was by maintaining the linear velocity (v) in a pipe around 3.5–4 m/s and Reynolds (Re) number above 21,000. At this value the maximum shear rate exerted by the flowing fluid is in the range of 24–35 s^{-1} for both of the impeller orientation (Fig. 4). At this value the shear force exerted by the fluid on settled particles dominates the attractive force between the metal surface and the crystals and the scale deposition is completely inhibited. On further increasing the shear rate, erosion of the metal surface prevails. Hence, the shear rate has to be operated within the optimized range 24–35 s^{-1}.

References

1. Z. Amjad, R. T. Landgraf and J. L. Penn, *Int. J. Corros. Scale Inhib.*, 2014, **3(1)**, 35.
2. S. Muryanto, A. P. Bayuseno, H. Ma'mun, M. Usamah and Jotho, *Procedia Chemistry*, 2014, **9**, 69.
3. S. Z. Ansari and A. B. Pandit, *Indian Chem. Eng.*, 2019.
4. "The Corrosion and Scale Handbook", Elsevier Inc, 2015, p. 207.
5. J. Macadam and S. A. Parsons, *Rev. Environ. Sci. Bio/Technology*, 2004, Vol. 1, Chapman, 1992, pp. 159-169.
6. D. A. Roberts, E. L. Johnston and N. A. Knott, 2010, **4**.
7. S. Lattemann and T. Höpner, *Desalination*, 2008, **220**, 1.
8. J. A. Camargo and Á. Alonso, *Environment International*, 2006, **32**, 831.
9. M. Chaussemier, *et al.*, *Desalination*, 2015, **356**, 47.
10. N. M. Kumar and K. Kanny, O*pen Journal of Organic Polymer Materials*, 2013, **2013(4)**, 53.
11. S. Z. Ansari and A. B. Pandit, *Chem. Eng. Process. – Process Intensif.*, 2020, **147**.
12. A. Quddus and L. M. Al-hadhrami, *Desalin. Water Treat.*, 2012, December 2014, pp. 37-41.
13. A. Quddus, *Desalination*, 2002, **142**, 57.
15. I. M. A. A. Quddus, *Desalination*, 2000, **127**, 219.
16. P. Research, *Pine Res. Instrum.*, 2016, **3**, 1.
17. Tulus, Mardiningsih, Sawaluddin, O. S. Sitompul and A. K. A. M. Ihsan, *IOP Conf. Ser. Mater. Sci. Eng.*, 2018, **308(1)**.
19. C. Johnston, L. Sutherland, N. Champion and T. Herrman, *SPE International*, 2014, 169760-MS.
20. V. Santos-Moreau, L. Brunet-Errard and M. Rolland, *Chem. Eng. J.*, 2012, **207-208**, 596.
21. A. Campesi, M. O. Cerri, C. O. Hokka and A. C. Badino, *Bioprocess Biosyst. Eng.*, 2009, **32(2)**, 241.
22. S. Nagata, Halsted Press, 1975, pp. 30-50.
23. J. Y. Oldshue, 1983, pp. 40-60.